

A review of airborne laser bathymetry for mapping of inland and coastal waters

A peer-reviewed paper by GOTTFRIED MANDLBURGER

Airborne laser bathymetry (ALB), an active remote sensing technique for capturing the depth and topography of shallow inland and coastal waters, is continuously evolving due to technological progress concerning sensors, platforms and data processing methods. So-called deep bathy systems with low spatial resolution but high depth penetration of up to 60 m coexist with topo-bathymetric sensors featuring small laser footprints of around 50 cm, high measurement point density of more than 20 points/m² but limited depth penetration of about 1.5 Secchi depths. While conventional ALB sensors are typically mounted on manned aircraft and operated from flying altitudes of around 500 m, sensor miniaturisation enabled the integration of compact bathymetric laser scanners on agile unmanned aerial vehicles (UAV) operated from 50 to 150 m altitude for flexible acquisition of smaller water bodies like clear gravel-bed rivers. This in turn, initiated new applications like roughness estimation, mapping of benthic habitats, and monitoring of coastal and fluvial morpho-dynamics in high spatial and temporal resolution. Furthermore, new data processing approaches proved to enhance both accuracy and depth penetration via strict geometric modelling and sophisticated waveform processing. The paper reviews the current trends in airborne laser bathymetry and highlights the potential and restriction of this optical technique.

bathymetric LiDAR | green laser | laser scanning | ALB sensors | ALB platforms
bathymetrisches LiDAR | grüner Laser | Laserscanning | ALB-Sensoren | ALB-Plattformen

Die luftgestützte Laserbathymetrie (ALB) ist eine aktive Fernerkundungstechnik, mit der sich die Tiefe und Topographie von flachen Binnen- und Küstengewässern erfassen lässt und die sich aufgrund des technologischen Fortschritts bei Sensoren, Plattformen und Datenverarbeitungsmethoden ständig weiterentwickelt. Neben sogenannten Tiefwassersystemen mit geringer räumlicher Auflösung, aber hoher Eindringtiefe von bis zu 60 m gibt es topo-bathymetrische Sensoren, die kleine Footprints von etwa 50 cm und eine hohe Messpunktdichte von mehr als 20 Punkten/m² aufweisen, aber nur eine begrenzte Eindringtiefe von etwa 1,5 Secchi-Tiefen. Während herkömmliche ALB-Sensoren typischerweise auf bemannten Flugzeugen montiert sind und aus Flughöhen von etwa 500 m betrieben werden, ermöglichte Sensorminiaturisierung die Integration kompakter bathymetrischer Laserscanner auf agilen unbemannten Luftfahrzeugen (UAV), wodurch kleinere Wasserkörper wie klare Flüsse mit Kieselbett aus einer Flughöhe von 50 bis 150 m flexibel erfasst werden können. Dies wiederum ermöglichte neue Anwendungen wie die Schätzung der Rauigkeit, die Kartierung benthischer Lebensräume und die Überwachung der Morphodynamik von Küstengewässern und Flusssystemen in hoher räumlicher und zeitlicher Auflösung. Darüber hinaus verbesserten neue Datenverarbeitungsansätze durch strenge geometrische Modellierung und hochentwickelte Wellenformverarbeitung sowohl die Genauigkeit als auch die Eindringtiefe. Der Beitrag gibt einen Überblick über die aktuellen Trends in der luftgestützten Laserbathymetrie und zeigt das Potenzial und die Einschränkungen dieser optischen Technik auf.

Author

Dr. Gottfried Mandlbürger is a Senior Researcher at TU Wien, Department of Geodesy and Geoinformation.

gottfried.mandlbuerger@geo.tuwien.ac.at

1 Introduction

Airborne laser bathymetry (ALB), also referred to as airborne laser hydrography (ALH), is a technique for measuring the depths of relatively shallow coastal and inland water bodies with a pulsed scanning laser from the air (Guenther et al. 2000). The employed lasers are operating in the visible green domain of the electromagnetic spectrum ($\lambda = 532$ nm) and the depths are determined by measuring the round trip time of short laser pulses reflected from the bottom of the water body after traveling through the atmosphere and the water

column. Additional reflections from the air-water-interface are used to reconstruct the 3D-shape of the water surface. Exact knowledge of the height and tilt of the water surface is a precondition to correct the raw measurement due to refraction effects at the air-water-interface (Westfeld et al. 2017; Birkebak et al. 2018; Richter et al., 2018).

The measurable depth of this active remote sensing technique mainly depends on the optical properties of the water body (i.e. turbidity). State-of-the-art bathymetric sensors can measure depths in the range of 1 to 3 times the Secchi

depth (SD), corresponding to 20 to 60 m for clear coastal waters with a diffuse attenuation coefficient of $k < 0.1$ (Guenther 1985; Mobley 1994). In addition to depth and bottom topography, ALB allows the estimation of turbidity by analysing the full waveform (FWF) of the backscattered laser pulses (Abdallah et al. 2012; Richter et al. 2017; Zhao et al. 2018). It is noted that in this context the term full waveform denotes the temporal record of the received laser signal amplitude (Wagner 2010) rather than the shape of water waves.

Whereas traditional hydrographic mapping via sonar (sound navigation and ranging) yields a higher penetration depth (>100 m), ALB is well suited for capturing the shallow near shore area (Guenther et al. 2000) as well as unnavigable and ecologically sensitive areas with restricted access (Pfennigbauer et al. 2011). This article provides a compact airborne laser bathymetry review and is structured as follows: Section 2 introduces the basic principles of ALB. Section 3 discusses available sensor and platform concepts and section 4 lists potential applications. The article concludes with a summary and remarks on current trends in section 5.

2 Basics of airborne laser bathymetry

The principles of ALB are summarised in Pfeifer, Mandlburger and Glira (2015) and in Philpot (2019). Fig. 1 shows a conceptual drawing of the measurement process. A short laser pulse in the green domain of the spectrum ($\lambda = 532$ nm) is emitted from the scanner mounted on an aerial platform (aircraft, helicopter, UAV, etc.), travels through the atmosphere and hits the water surface, where a part of the signal is scattered back. The remaining part propagates through the water column with reduced propagation speed, is reflected from the water bottom, and a small portion of the emitted laser power reaches the sensor's receiver after the return trip. Based on the time-of-flight principle ranges are derived from the round trip time, i.e., the time span between pulse emission and arrival of the backscattered echo pulse. In ALB, the complete waveform of the backscattered signal is digitised with high temporal resolution (typically 0.5 ns). Pulse detection is achieved by analysing the full echo waveform either online in the instrument (Pfennigbauer et al. 2014) or in post processing (Allouis et al. 2010; Abady et al. 2014; Schwarz et al. 2019). Surface and bottom detection is exemplified in the sketch of the received echo waveform in Fig. 1 as two gray Gaussian curves.

ALB is a multimedia measurement technique with the laser pulses travelling in air and water. The two media are characterised by their refractive indices n_{air} and n_{water} describing the relative signal propagation speed in vacuum (c_0) and the respective media (c_{air} , c_{water}). At the air-water-interface the laser beam gets deflected and the

propagation speed reduces. Both beam deflection and change of signal propagation velocity are described by Snell's law:

$$\frac{\sin \alpha_{\text{air}}}{\sin \alpha_{\text{water}}} = \frac{c_{\text{air}}}{c_{\text{water}}} = \frac{n_{\text{water}}}{n_{\text{air}}}$$

$$\text{With: } n_{\text{air}} = c_0/c_{\text{air}} \approx 1.0 \\ n_{\text{water}} = c_0/c_{\text{water}} \approx 1.33$$

To ensure eye safe operation, green laser beams are generally broader compared to infrared (IR) lasers used for topographic application. Typical laser beam divergences range from 1 to 7 mrad resulting in a diameter of the illuminated footprint area at the water surface of 50 to 350 cm for a nominal flying altitude of 500 m. Further non-linear beam spreading takes place in the water column caused by volume scattering at floating and suspended particles (cf. hyperbolic underwater light cone, Fig. 1). Signal attenuation in water is exponential as a result of scattering and absorption and leads to asymmetric shapes of the received echo waveform (Tulldahl and Steinvall 2004; Abdallah et al. 2012). Typical water waveforms show a first peak from the water surface, followed by an asymmetric descent in the water column and a weak response from the water bottom. Next to the receiver sensitivity, the maximum penetration capability of any ALB system is limited by the water optical properties, i.e., turbidity, which is described either by the diffuse attenuation coefficient k or the Secchi depth SD (Guenther 1985; Guenther et al. 2000).

The attenuation coefficient k appears as the exponent in the water column term of the laser-radar-equation (Tulldahl and Steinvall 1999; Abdallah et al. 2012; Pfeifer, Mandlburger and Glira 2015) and, thus, influences the asymmetric signal decay in the received echo waveform. Turbid water conditions ($k = 1$) lead to a steeper signal decay compared to clear water ($k = 0.1$). SD is an empirical turbidity measure. It denotes the distance, where the black and white quadrants of a 20 cm or 30 cm checkerboard disk lowered into the water can no longer be distinguished. k and SD are approximately related by $SD \approx 1.6/k$ (ISO 2019). The most powerful bathymetric laser scanners feature a depth performance of approximately 3 SD . Thus, ALB is restricted to depths less than 60 m in very clear water conditions with $SD = 20$ m ($k = 0.08$). Such ideal conditions apply to certain coastal waters (e.g., Caribbean Sea) and calm sea state. In contrast, unfavourable environmental conditions (wind, thunderstorms, snow melt, etc.) entail higher suspended sediment concentration (SSC), which reduces the measurable depth to less than 10 m.

Precise knowledge of the 3D shape of the water surface is a prerequisite for applying refraction and run-time correction of the raw laser measurements which, in turn, is a precondition for obtain-

ing precise water depths and underwater topography (Thomas and Guenther 1990; Guenther et al. 2000). When using green laser radiation only, water surface returns always constitute a mixture of reflections from the surface and sub-surface volume backscattering (Guenther 1986; Guenther et al. 2000). This typically leads to water level underestimation (Mandlbauer 2017). Thus, traditional ALB systems use an additional non-water penetrating IR laser, synchronously and collinearly emitted with the green laser to capture the shape of the water surface. Today, most instruments abdicate the use of a co-aligned IR laser and either use a separate IR scanner as depicted in Fig. 1 or entirely drop the IR channel and estimate the water surface from the

green laser returns only. In the latter case, sophisticated waveform modelling (Schwarz et al. 2019) or spatial aggregation (Mandlbauer, Pfennigbauer and Pfeifer 2013) are necessary to minimise systematic water surface underestimation. Surface model simplification, however, limits the achievable depth accuracy and leads to systematic errors (Westfeld et al. 2017; Richter et al. 2018).

Apart from these bathymetry specific and pulse related tasks (surface and bottom echo detection, refraction and run time correction, etc.), 3D point cloud generation is identical to the topographic case. In a process referred to as direct georeferencing, scanner measurements (range, scan angle) are combined with position and attitude information

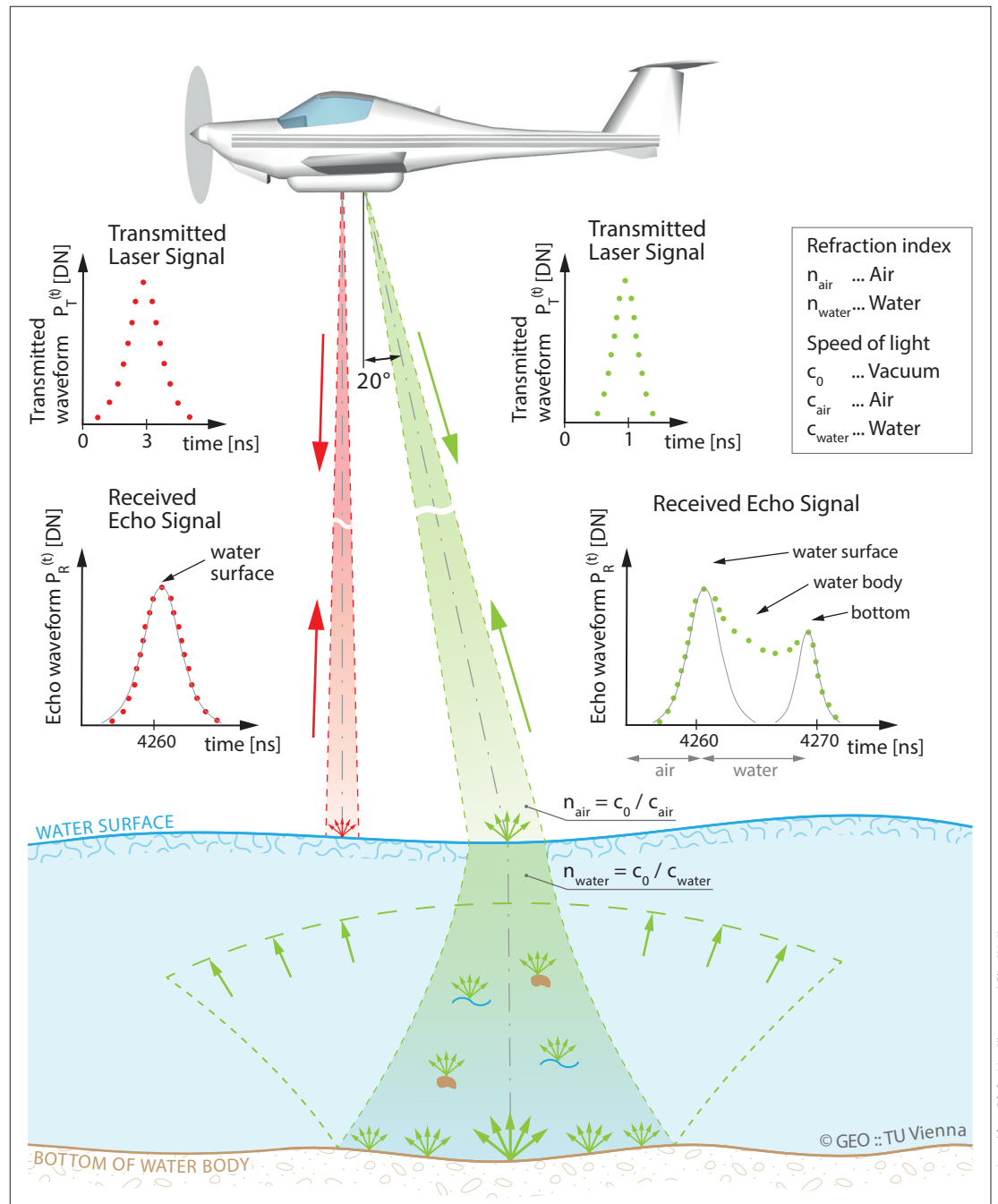


Fig. 1: Conceptual drawing of the principle of airborne laser bathymetry

Figure adapted from Pfeifer, Mandlbauer and Gira (2015)

from a navigation device consisting of a global navigation satellite system (GNSS) receiver and an inertial measurement unit (Vosselman and Maas 2010; Shan and Toth 2018).

3 Sensors and platforms

ALB systems can be categorised into deep bathymetric, topo-bathymetric, and multi-purpose sensors. The aim of deep bathymetric scanners is maximising depth penetration for mapping coastal waters. These systems utilise relatively long and broad laser pulses (pulse duration: 7 ns, beam divergence: 7 mrad), high pulse energy (7 mJ), and a low measurement rate (3 to 10 kHz) entailing large laser footprints and low point density. Capturing smaller inland waters, in turn, requires higher spatial resolution. Therefore, state-of-the-art topo-bathymetric sensors use short and narrow laser beams (pulse duration: 1 to 2 ns, beam divergence: 0.7 to 2 mrad) and higher pulse repetition rates of up to 500 kHz resulting in laser footprint diameters of 0.5 to 1 m and a point density of around 20 points/m². Topo-bathymetric scanners, however, only feature a maximum penetration of around 1.5 SD. In the recent years, multi-spectral and single photon LiDAR scanners were introduced in the market. The prior enable the derivation of vegetation indices featuring both infrared and green laser wavelengths (Fernandez-Diaz et al. 2016) and the latter is primarily used for large scale topographic mapping (Degnan 2016), but both also feature bathymetric capabilities. Single photon technology is also used by the LiDAR instrument aboard the ICESat-2 satellite (Parish et al. 2019).

Apart from depth penetration, ALB systems differ with reference to the utilised laser wavelengths. As stated before, traditional ALB systems utilise coaxial infrared and green laser beams for water surface and water bottom detection on a

per pulse basis (Wozencraft and Lillycrop 2003; Fuchs and Tuell 2010). Other sensors use disjoint infrared and green lasers (cf. Fig. 1), resulting in precise reconstructions of static water surfaces from the non-water penetrating infrared channel. Many of today’s instruments, however, use green lasers only to detect both water surface and bottom (Pfennigbauer et al. 2011; Wright et al. 2016). This poses challenges for water surface modelling, as laser echoes from the water surface constitute a mixture of specular reflections from the air-water interface and sub-surface volume backscattering, which demands sophisticated data processing for obtaining precise water surface models (Thomas and Guenther 1990; Birkebak et al. 2018; Mandlbürger et al. 2013; Schwarz et al. 2019).

Another possibility for categorising ALB sensors is the carrier platform. While deep bathymetric systems are typically bulky with a weight of 50 to 100 kg and require larger aircraft, topo-bathymetric systems are more compact in size and weight and can be integrated in light aircraft and helicopters. Ongoing sensor miniaturisation currently leads to the development of lightweight bathymetric laser scanners (5 to 15 kg) suitable for integration in gyrocopters, helicopters and even unmanned aerial vehicles (UAV).

Table 1 summarises the key parameters of different deep bathymetric and topo-bathymetric sensors. The reported pulse energy, pulse duration, beam divergence and depth penetration values always refer to the bathymetric channels. If more than one green laser channel is available (HawkEye 4X, CZMIL Nova, EAARL-B), the values refer to the deep water channel. Although deep and shallow water channels both use the same laser wavelength ($\lambda = 532$ nm), the higher penetration depth of the deep water channels is generally achieved by using higher pulse energy, longer pulse dura-

	LADS HD	HawkEye 4X	CZMIL Nova	VQ-880-GII	Chiroptera 4X	EAARL-B
	deep bathymetric			topo-bathymetric		
Weight [kg]	n/s	~170	290	65	n/s	n/s
Dimensions [cm]	n/s	n/s	89 × 60 × 90	52 × 52 × 69	~67 × 53 × 75	n/s
Laser channels [nm]	532	532/532/1064	532/532/1064	532/1064	532/1064	532/532
Camera	RGB + hypersp	RGBI	RGB + hypersp	RGB	RGBI	---
Measurement rate [kHz]	3.0	40/140/500	10/70/80	700/279	140/500	15–30
Pulse energy [mJ]	7	3	4	n/s	0.1	0.4/0.13
Pulse duration [ns]	~7	2	3	1.5	4	1.3
Field of view [°]	n/s	40	40	40	40	44
Beam divergence [mrad]	7	7	7	0.7–2	~3	1
Nominal flying altitude [m]	365–900	400–600	400–1000	600–700	400–600	300
Laser footprint [cm]	270–630	280–420	280–700	40–280	120–180	30
Scan pattern	rectilinear	elliptical	circular	circular	elliptical	elliptical arc
Depth performance [SD]	3.0	3.0	3.0	1.5	1.7	2.5

Table 1: Key parameters of deep bathymetric and topo-bathymetric laser scanners

	BDF-1	ASTRALite	RAMSS	VQ-840-G
Weight [kg]	5.3	5.0	14	12
Dimensions [cm]	45 × 18 × 14	27 × 23 × 19	~42 × 37 × 760	36 × 29 × 20
Camera	RGB	---	RGB	RGB
Measurement rate [kHz]	4	20	25	50–200
Pulse duration [ns]	1.2	n/s	5.1	1.5
Field of view [°]	n/s	30	45	40
Beam divergence [mrad]	n/s	12	n/s	1–6
Flying altitude [m]	20	20	325	50–150
Laser footprint [cm]	3.5	24	n/s	5–90
Scan mechanism	no scanning	rectilinear	pushbroom	elliptical
Depth performance [SD]	1.5	1.5	3.0	2.0

Table 2: Key parameters of bathymetric UAV-laser sensors

tion and a larger beam divergence. Table 1 clearly shows that the deep water systems provide a maximum penetration depth of around 3 SD but feature a large laser footprint diameter in the range of 3 to 7 m and a moderate measurement rate of 3 to 40 kHz resulting in point densities of ≤ 2 points/m². The topo-bathymetric scanners and the shallow water channels of deep bathymetric scanners, in turn, are optimised for high resolution mapping. They feature smaller footprint diameters in the m-range, higher measurement rates of up to 700 kHz resulting in a water bottom point density of around 20 points/m² at the price of limited depth penetration capability (1.5 SD). Most of the sensors are equipped with RGB cameras for the prime purpose of photo documentation. Some instruments, however, also integrate high-resolution metric cameras (e.g. PhaseOne IXU, RDC30) allowing bathymetric mapping also from concurrently captured images via multimedia stereo photogrammetry (Westaway, Lane and Hicks 2001; Maas 2015; Mandlbürger 2019) or spectrally based depth estimation (Lyzenga, Malinas and Tanis 2006; Legleiter, Dar and Rick 2009).

Deep water channels generally use high energy laser pulses which require powerful laser sources on the one hand and longer pulse durations on the other hand. The latter has an implication concerning the minimum detectable depth, as surface and bottom echoes conflate to a single peak in the received waveform. For this reason, topo-bathymetric scanners dedicated to shallow water mapping generally use very short laser pulses of around 1 ns. This is especially important for green-only instruments. Concerning vertical accuracy, all LiDAR instruments listed in Table 1 meet the required accuracy standards formulated by the International Hydrographic Organization (IHO 2008). The standard defines different levels of accuracy demand (orders), among which the special order is the most rigorous requiring a total vertical uncertainty (TVU) of better than 30 cm. This measure

includes all possible error factors like positioning, orientation, boresight alignment, ranging, as well as uncertainties related to water surface and water column (Eren et al. 2019).

Table 2 summarises the key parameters of the latest generation of compact bathymetric laser scanners which also allow integration on UAVs. These small and lightweight sensors are operated from 20 to 150 m resulting in smaller laser footprints in the dm-range. The generally high measurement rate of 20 to 200 kHz entails a point density of more than 50 points/m² which opens new possibilities for small object detection and roughness estimation (Mandlbürger et al. 2020). The depth measurement performance is on par or even better compared to topo-bathymetric sensors operated from manned platforms. In addition, the mobilisation costs are lower and the use of agile airborne platforms make these instruments especially well-suited for capturing medium sized rivers when integrated on UAV platforms but also for capturing coastal areas when integrated on light aircraft.

Fig. 2 shows selected ALB scanners featuring instruments with deep water channels (a, b), topo-bathymetric sensors designed for manned aircraft (a, b, c, d) and compact topo-bathymetric sensors designed for UAV-integration (e, f). Except f, all instruments feature digital cameras in addition to the LiDAR sensors and therefore fall into the category of hybrid mapping sensors.

4 Applications

The applications of ALB are manifold and constantly increasing as the available sensors are getting more versatile on the one side and more compact on the other side. In the following, some exemplary applications and related publications are listed.

- Underwater object detection: The first application of bathymetric LiDAR was underwater object detection for military purposes (Sorenson, Honey and Payne 1966). More recent civil application in the maritime domain include object detection for maintaining harbour security, safe navigation of autonomous underwater vehicles, and safety of the littoral zone (Matteoli et al. 2015). In any case, the detection of small objects requires sophisticated full waveform analysis (Tulldahl and Steinvall 1999). While ALB sensors operated from manned platforms feature footprint diameters in the m-range, detection and reconstruction of boulder-size objects became feasible with the introduction of UAV-borne laser bathymetry (Mandlbürger et al. 2020).
- 3D-mapping of submerged topography: This is the main application of ALB. Hickman and Hogg (1969) were the first to confirm the general feasibility to perform laser-based near-shore hydrography. Since then, ALB was increasingly used for nautical charting in shal-



Fig. 2: Examples of airborne laser bathymetry sensors. (a) Chiroptera 4X and HawkEye 4X, (b) CZMIL (Coastal Zone Mapping and Imaging Lidar), (c) VQ-880-GII, (d) Titan Multispectral Lidar, (e) VQ-840-G, (f) ASTRALite edgeLidar

low water coastal and harbour environments with a focus on maximising depth penetration (Guenther and Goodman 1978; Guenther et al. 2000; Wozencraft and Lillycrop 2003; Song et al. 2015). Most recently, even space-borne instruments like ICESat-2 proved its suitability for near-shore bathymetric mapping (Parrish et al. 2019). For mapping smaller inland water bodies, the higher spatial resolution offered by topo-bathymetric LiDAR sensors operated from manned and unmanned platforms is required (Mitchell, Thayer and Hayman 2010; Pfennigbauer et al. 2011; Doneus et al. 2013; Kinzel, Legleiter and Nelson 2013; Fernandez-Diaz et al. 2014; Legleiter et al. 2016; Steinbacher et al. 2016; Kasvi et al. 2019; Mader et al. 2019; Mitchell 2019). Today, the progress in charting of submerged topography via ALB profits from systematic integration into regional and national mapping programs (Wessels et al. 2015; Christiansen 2016; Danielson et al. 2016; Ellmer 2016; Witmer et al. 2016).

- Ecology: Environmental applications of ALB are strongly promoted by trans-national initiatives and frameworks all over the world, but especially in Europe (European Commission 1992, 2000, 2007). This applies to the coastal zone as well as to inland lakes and running waters. Applications concentrate on estimation of seafloor

reflectance and detection, classification, and modelling of benthic habitats (Wedding et al. 2008; Aitken et al. 2010; Mandlbürger et al. 2015; Parrish et al. 2016; Wilson et al. 2019). Another important aspect in this context is river restoration (Kinzel, Legleiter and Nelson 2013; Miller and Addy 2019).

- Coastal and fluvial geomorphology: ALB is increasingly used in geomorphology studies both for understanding the impact of long-term processes as well as short-term fluctuations caused by hydropeaking (Fink et al. 2005; Fink and Andrews 2009; Hauer and Pulg 2018; Juárez et al. 2019). It is also gaining importance as the prime basis for all kinds of hydrodynamic-numerical models and flow related applications (McKean et al. 2014; Mandlbürger et al. 2015; Kinzel and Legleiter 2019; Tonina et al. 2019).
- Turbidity estimation: The main factor limiting depth penetration in ALB is turbidity. Beyond that, water turbidity itself is an important factor as a proxy for water quality. Regular monitoring is, e.g., requested by the European Water Frame Directive (European Commission 2000). An increasing body of literature documents the feasibility of ALB-derived turbidity estimation based on sophisticated full waveform analysis (Steinbacher et al. 2016; Richter et al. 2017; Zhao et al. 2018; Launeau et al. 2019).

- Risk assessment and disaster management: Driven by climate change, the increased occurrence of extreme weather phenomena (thunderstorms, hurricanes, floods, etc.) require up-to-date data of pre and post states of coastal and alluvial areas, both above and below the water table. While it is clear that this requirement can only be fulfilled by combining all sorts of acquisition techniques, ALB plays an important role in this context (Zhang et al. 2005; Robertson 2007; Parrish et al. 2016; Eisemann et al. 2019).

5 Summary and outlook

In this article, the basics and potential applications of airborne laser bathymetry were reviewed. This active, optical, multimedia remote sensing technique uses short laser pulses in the green domain of the spectrum to estimate the depth of relatively clear and shallow coastal and inland water bodies via round trip time measurement. One of the core steps for processing bathymetric LiDAR data is refraction and run-time correction of the raw laser signals, as the laser beam is subject to beam deflection at the air-water-interface and the laser pulses travel with reduced propagation speed in water. Precise modelling of the water surface and bottom as well as characterisation of the water column properties require understanding of the complex interaction of laser radiation with the medium water and are enabled by elaborate full waveform analysis.

Today, ALB sensors are operated from manned and unmanned platforms. State-of-the-art scanners provide a deep as well as a shallow water channel. Whereas the prior is optimised for maximum depth penetration of up to 3 SD with limited spatial resolution, the latter features high spatial resolution with typical laser footprint diameters of around 50 cm and a laser pulse density of up to 20 points/m² with limited depth penetration

of 1.5 SD. Turbidity is the main parameter limiting depth penetration. In very clear waters, deep water systems can reach a maximum depth of around 60 m. Thus, ALB is restricted to shallow water areas but constitutes an alternative to sonar hydrography in the very shallow zone, where shipborne acquisition is both dangerous and less efficient. ALB and sonar should, therefore, rather be considered complementary than competing bathymetric mapping techniques.

Ongoing sensor and platform miniaturisation has just recently enabled integration of bathymetric LiDAR on UAV platforms. The agility of UAVs together with the higher spatial resolution in the dm-range enable new applications of ALB like roughness characterisation as well as detection and 3D reconstruction of small submerged features and objects. This expands the potential field of use of ALB which today include bathymetric mapping of coastal and inland waters, detection of submerged objects, coastal and fluvial geomorphology, ecology including aquatic habitat modelling and river restoration, flood risk assessment, disaster management, and the like.

The recent generation of hybrid sensors comprising bathymetric laser scanners and multispectral cameras furthermore enables joint processing of data from active and passive sources. Thus, the originally distinct fields of laser bathymetry, multimedia photogrammetry, and spectrally based depth estimation are currently coalescing. While image-based techniques for deriving bathymetry are limited to the visual depth (i.e., 1 SD), lasers provide a higher depth penetration, but inherent physical limits also apply to ALB due to light attenuation in water. Thus, today's challenges for maintaining and improving the complex and sensitive shallow and deep water ecosystem require intensified collaboration of experts in the field of sonar hydrography and LiDAR bathymetry. //

References

- Abady, Lydia; Jean Stéphane Bailly et al. (2014): Assessment of quadrilateral fitting of the water column contribution in lidar waveforms on bathymetry estimates. *IEEE Geoscience and Remote Sensing Letters*, DOI: 10.1109/LGRS.2013.2279271
- Abdallah, Hani; Nicolas Baghdadi et al. (2012): Wa-LiD: A new LiDAR simulator for waters. *IEEE Geoscience Remote Sensing Letters*, DOI: 10.1109/LGRS.2011.2180506
- Aitken, Jennifer; Vinod Ramnath et al. (2010): Prelude to CZMIL: Seafloor imaging and classification results achieved with CHARTS and the Rapid Environmental Assessment (REA) processor. *Algorithms and Technologies for Multispectral, Hyperspectral, and Ultraspectral Imagery*, DOI: 10.1117/12.851915
- Allouis, Tristan; Jean-Stéphane Bailly et al. (2010): Comparison of LiDAR waveform processing methods for very shallow water bathymetry using raman, near-infrared and green signals. *Earth Surface Processes and Landforms*, DOI: 10.1002/esp.1959
- Birkebak, Matthew; Firat Eren et al. (2018): The effect of surface waves on Airborne Lidar Bathymetry (ALB) measurement uncertainties. *Remote Sensing*, DOI: 10.3390/rs10030453
- Christiansen, Lutz (2016): New techniques in capturing and modelling of morphological data. *Hydrographische Nachrichten*, DOI: 10.23784/HN105-04
- Danielson, Jeffrey J.; Sandra K. Poppenga et al. (2016): Topo-bathymetric elevation model development using a new methodology: Coastal National Elevation Database. *Journal of Coastal Research*, DOI: 10.2112/si76-008
- Degnan, John J. (2016): Scanning, multibeam, Single Photon Lidars for rapid, large scale, high resolution, topographic

- and bathymetric mapping. *Remote Sensing*, DOI: 10.3390/rs8110958
- Doneus, Michael; Nives Doneus et al. (2013): Airborne Laser Bathymetry – Detecting and recording submerged archaeological sites from the air. *Journal of Archaeological Science*, DOI: 10.1016/j.jas.2012.12.021
- Eisemann, Eve; Lauren Dunkin et al. (2019): JALBTCX/NCMP Emergency-Response Airborne Lidar Coastal Mapping & Quick Response Data Products for 2016/2017/2018 Hurricane Impact Assessments. *Shore & Beach*, DOI: 10.34237/1008744
- Ellmer, Wilfried (2016): Use of laser bathymetry at the German Baltic Sea coast. *Hydrographische Nachrichten*, DOI: 10.23784/HN105-05
- Eren, Firat; Jaehoon Jung et al. (2019): Total Vertical Uncertainty (TVU) modeling for topo-bathymetric LIDAR systems. *Photogrammetric Engineering and Remote Sensing*, DOI: 10.14358/PERS.85.8.585
- European Commission (1992): Council Directive 92/43/EEC on the Conservation of Natural Habitats and of Wild Fauna and Flora. *Official Journal of the European Communities (OJL) L 206 (35)*
- European Commission (2000): Directive 2000/60/EC of the European Parliament and of the Council of 23 October 2000 Establishing a Framework for Community Action the Field of Water Policy. *Official Journal of the European Communities (OJL) L 327 (173): 1–72*
- European Commission (2007): Directive 2007/60/EC of the European Parliament and European Council of October 2007 on the Assessment and Management of Flood Risks. *Official Journal of the European Communities (OJL) 288 (27)*
- Fernandez-Diaz, Juan Carlos; Craig L. Glennie et al. (2014): Early results of simultaneous terrain and shallow water bathymetry mapping using a single-wavelength airborne LIDAR sensor. *IEEE Journal Of Selected Topics in Applied Earth Observations and Remote Sensing*, DOI: 10.1109/JSTARS.2013.2265255
- Fernandez-Diaz, Juan Carlos; William E. Carter et al. (2016): Capability assessment and performance metrics for the Titan Multispectral Mapping Lidar. *Remote Sensing*, DOI: 10.3390/rs8110936
- Fink, Charles W.; Lindino Benedet; Jeffrey L. Andrews (2005): Interpretation of seabed geomorphology based on spatial analysis of high-density airborne laser bathymetry. *Journal of Coastal Research*, DOI: 10.2112/05-756A.1
- Fuchs, Eran; Grady Tuell (2010): Conceptual design of the CZMIL Data Acquisition System (DAS): Integrating a new bathymetric Lidar with a commercial spectrometer and metric camera for coastal mapping applications. *Algorithms and Technologies for Multispectral, Hyperspectral, and Ultraspectral Imagery*, DOI: 10.1117/12.851919
- Guenther, Gary (1985): Airborne Laser Hydrography: System design and performance Factors. *NOAA Professional Paper Series*
- Guenther, Gary (1986): Wind and nadir angle effects on airborne Lidar water surface returns. *Proceedings SPIE*, DOI: 10.1117/12.964243
- Guenther, Gary; Lowell R. Goodman (1978): Laser applications for near-shore nautical charting. *Ocean Optics V*, DOI: 10.1117/12.956863
- Guenther, Gary; Grant Cunningham et al. (2000): Meeting the accuracy challenge in airborne Lidar bathymetry. *Proceedings of the 20th EARSel Symposium: Workshop on Lidar Remote Sensing of Land and Sea*. Dresden, Germany
- Hauer, Christoph; Ulrich Pulg (2018): The non-fluvial nature of western Norwegian rivers and the implications for channel patterns and sediment composition. *Catena 171*, DOI: 10.1016/j.catena.2018.06.025
- Hickman, G. Daniel; John E. Hogg (1969): Application of an airborne pulsed laser for near shore bathymetric measurements. *Remote Sensing of Environment*, DOI: 10.1016/S0034-4257(69)90088-1
- IHO (2008): S-44, Standards for hydrographic surveys. www.iho.int/iho_pubs/standard/S-44_5E.pdf
- ISO (2019): Water Quality – Determination of turbidity – Part 2: Semi-quantitative methods for the assessment of transparency of waters. www.iso.org/standard/69545.html
- Juárez, Ana; Ana Adeva-Bustos et al. (2019): Performance of a two-dimensional hydraulic model for the evaluation of stranding areas and characterisation of rapid fluctuations in hydropeaking rivers. *Water (Switzerland)*, DOI: 10.3390/w11020201
- Kasvi, Elina; Jouni Salmela et al. (2019): Comparison of remote sensing based approaches for mapping bathymetry of shallow, clear water rivers. *Geomorphology*, DOI: 10.1016/j.geomorph.2019.02.017
- Kinzel, Paul J.; Carl J. Legleiter (2019): SUAS-based remote sensing of river discharge using thermal particle image velocimetry and bathymetric Lidar. *Remote Sensing*, DOI: 10.3390/rs11192317
- Kinzel, Paul J.; Carl J. Legleiter; Jonathan M. Nelson (2013): Mapping river bathymetry with a small footprint green LiDAR: Applications and challenges. *JAWRA Journal of the American Water Resources Association*, DOI: 10.1111/jawr.12008
- Launeau, Patrick; Manuel Giraud et al. (2019): Full-waveform LiDAR fast analysis of a moderately turbid bay in Western France. *Remote Sensing*, DOI: 10.3390/rs11020117
- Legleiter, Carl J.; Brandon T. Overstreet et al. (2016): Evaluating the capabilities of the CASI Hyperspectral Imaging System and Aquarius Bathymetric LiDAR for measuring channel morphology in two distinct river environments. *Earth Surface Processes and Landforms*, DOI: 10.1002/esp.3794
- Legleiter, Carl J.; A. Roberts Dar; L. Lawrence Rick (2009): Spectrally based remote sensing of river bathymetry. *Earth Surface Processes and Landforms*, DOI: 10.1002/esp.1787
- Lyzenga, David R.; Norman P. Malinas; Fred J. Tanis (2006): Multispectral bathymetry using a simple physically based algorithm. *IEEE Transactions on Geoscience and Remote Sensing*, DOI: 10.1109/TGRS.2006.872909
- Maas, Hans-Gerd (2015): On the accuracy potential in underwater/multimedia photogrammetry. *Sensors*, DOI: 10.3390/s150818140
- Mader, David; Katja Richter et al. (2019): Detection and extraction of water bottom topography from laser bathymetry data by using full-waveform stacking techniques. *ISPRS – International Archives of the Photogrammetry, Remote Sensing and Spatial Information Sciences*, DOI: 10.5194/isprs-archives-XLII-2-W13-1053-2019
- Mandlbürger, Gottfried (2017): Interaction of laser pulses with the water surface – Theoretical aspects and experimental

- results. AVN Allgemeine Vermessungs-Nachrichten, 124, pp. 11–12
- Mandlbürger, Gottfried (2019): Through-water dense image matching for shallow water bathymetry. *Photogrammetric Engineering and Remote Sensing*, DOI: 10.14358/PERS.85.6.445
- Mandlbürger, Gottfried; Christoph Hauer et al. (2015): Topo-bathymetric LiDAR for monitoring river morphodynamics and instream habitats – A case study at the Pielach river. *Remote Sensing*, DOI: 10.3390/rs70506160
- Mandlbürger, Gottfried; Martin Pfennigbauer; Norbert Pfeifer (2013): Analyzing near water surface penetration in laser bathymetry – A case study at the river Pielach. *ISPRS Annals of the Photogrammetry, Remote Sensing and Spatial Information Sciences*, DOI: 10.5194/isprsannals-II-5-W2-175-2013
- Mandlbürger, Gottfried; Martin Pfennigbauer et al. (2020): Concept and performance evaluation of a novel UAV-borne topo-bathymetric LiDAR sensor. *Remote Sensing*, DOI: 10.3390/rs12060986
- Matteoli, Stefania; Giovanni Corsini et al. (2015): Automated underwater object recognition by means of fluorescence LiDAR. *IEEE Transactions on Geoscience and Remote Sensing*, DOI: 10.1109/TGRS.2014.2322676
- McKean, James; Daniele Tonina et al. (2014): Effects of bathymetric Lidar errors on flow properties predicted with a multi-dimensional hydraulic model. *Journal of Geophysical Research: Earth Surface*, DOI: 10.1002/2013JF002897
- Miller, Pauline; Stephen Addy (2019): Topo-bathymetric Lidar in support of hydromorphological assessment, river restoration and flood risk management. www.crew.ac.uk/publication/topo-bathymetric-lidar-support-hydromorphological-assessment-river-restoration-and-flood
- Mitchell, Steven; Jeffrey P. Thayer; Matthew Hayman (2010): Polarization Lidar for shallow water depth measurement. *Applied Optics*, DOI: 10.1364/AO.49.006995
- Mitchell, Todd (2019): From PILLS to RAMMS. 20th Annual JALBTCX Airborne Coastal Mapping and Charting Technical Workshop
- Mobley, Curtis (1994): *Light and water: radiative transfer in natural waters*. Academic Press
- Parrish, Christopher E.; Lori A. Magruder et al. (2019): Validation of ICESat-2 ATLAS bathymetry and analysis of ATLAS's bathymetric mapping performance. *Remote Sensing*, DOI: 10.3390/rs11141634
- Parrish, Christopher E.; Jennifer A. Dijkstra et al. (2016): Post-sandy benthic habitat mapping using new topobathymetric Lidar technology and object-based image classification. *Journal of Coastal Research*, DOI: 10.2112/SI76-017
- Pfeifer, Norbert; Gottfried Mandlbürger; Philipp Glira (2015): *Laserscanning*. *Photogrammetrie und Fernerkundung*, DOI: 10.1007/978-3-662-46900-2
- Pfennigbauer, Martin; Andreas Ullrich et al. (2011): High-resolution hydrographic airborne laser scanner for surveying inland waters and shallow coastal zones. *Proceedings SPIE*, DOI: 10.1117/12.883910
- Pfennigbauer, Martin; Clifford Wolf et al. (2014): Online waveform processing for demanding target situations. *Proceedings SPIE*, DOI: 10.1117/12.2052994
- Philpot, William (2019): *Airborne Laser Hydrography II*. Coernell, DOI: 10.7298/jxm9-g971
- Richter, Katja; Hans-Gerd Maas et al. (2017): An approach to determining turbidity and correcting for signal attenuation in airborne Lidar bathymetry. *Journal of Photogrammetry, Remote Sensing and Geoinformation Science*, DOI: 10.1007/s41064-016-0001-0
- Richter, Katja; David Mader et al. (2018): Numerical simulation and experimental validation of wave pattern induced coordinate errors in airborne Lidar bathymetry. *International Archives of the Photogrammetry, Remote Sensing and Spatial Information Sciences*, DOI: 10.5194/isprs-archives-XLII-2-961-2018
- Robertson, William (2007): *Airborne laser quantification of Florida shoreline and beach volume change caused by hurricanes*. ProQuest Dissertations and Theses, <https://search.proquest.com/docview/304711270?accountid=28155>
- Schwarz, Roland; Gottfried Mandlbürger et al. (2019): Design and evaluation of a full-wave surface and bottom-detection algorithm for LiDAR bathymetry of very shallow waters. *ISPRS Journal of Photogrammetry and Remote Sensing*, DOI: 10.1016/j.isprsjprs.2019.02.002
- Shan, Jie; Charles K. Toth (2018): *Topographic Laser Ranging and Scanning: Principles and Processing*. Taylor & Francis
- Song, Yujin; Joachim Niemeyer et al. (2015): Comparison of three airborne laser bathymetry data sets for monitoring the German Baltic Sea coast. *Proceedings SPIE*, DOI: 10.1117/12.2194960
- Sorenson, G. P.; R. C. Honey; J. R. Payne (1966): *Analysis of the use of airborne laser radar for submarine detection and ranging*. SRI Report 5583
- Steinbacher, Frank; Ramona Baran et al. (2016): High-resolution, topobathymetric LiDAR coastal zone characterisation. *Hydrographische Nachrichten* 105. DOI: 10.23784/HN105-03
- Thomas, Robert; Gary Guenther (1990): Water surface detection strategy for an airborne laser bathymeter. *Proceedings SPIE*, DOI: 10.1117/12.21474
- Tonina, Daniele; James McKean et al. (2019): Mapping river bathymetries: Evaluating topobathymetric LiDAR survey. *Earth Surface Processes and Landforms*, DOI: 10.1002/esp.4513
- Tulldahl, H. Michael; K. Ove Steinvall (1999): Analytical waveform generation from small Objects in Lidar bathymetry. *Applied Optics*, DOI: 10.1364/ao.38.001021
- Tulldahl, H. Michael; K. Ove Steinvall (2004): Simulation of sea surface wave influence on small target detection with airborne laser depth sounding. *Applied Optics*, DOI: 10.1364/AO.43.002462
- Vosselman, George; Hans-Gerd Maas (2010): *Airborne and Terrestrial Laser Scanning*. Whittles Publishing
- Wagner, Wolfgang (2010): Radiometric calibration of small-footprint full-waveform airborne laser scanner measurements: Basic physical concepts. *ISPRS Journal of Photogrammetry and Remote Sensing*, DOI: 10.1016/j.isprsjprs.2010.06.007
- Wedding, Lisa M.; Alan M. Friedlander et al. (2008): Using bathymetric Lidar to define nearshore benthic habitat complexity: Implications for management of reef fish assemblages in Hawaii. *Remote Sensing of Environment*, DOI: 10.1016/j.rse.2008.01.025
- Wessels, Martin; Flavio Anselmetti et al. (2015): Bathymetry of Lake Constance – A high-resolution survey in a large, deep

- lake. ZfV – Zeitschrift für Geodäsie, Geoinformation und Landmanagement, DOI: 10.12902/zfv-0079-2015
- Westaway, Richard M.; Stuart N. Lane; D. Murray Hicks (2001): Remote sensing of clear-water, shallow, gravel-bed rivers using digital photogrammetry. *Photogrammetric Engineering and Remote Sensing*, 67 (11), pp. 1271–1281
- Westfeld, Patrick; Hans-Gerd Maas et al. (2017): Analysis and correction of ocean wave pattern induced systematic coordinate errors in airborne LiDAR bathymetry. *ISPRS Journal of Photogrammetry and Remote Sensing*, DOI: 10.1016/j.isprsjprs.2017.04.008
- Wilson, Nicholas; Christopher E. Parrish et al. (2019): Mapping seafloor relative reflectance and assessing coral reef morphology with EAARL-B topobathymetric Lidar waveforms. *Estuaries and Coasts*, DOI: 10.1007/s12237-019-00652-9
- Witmer, Joshua D., Gretchen Imahori et al. (2016): Integration of U.S. Army Corps of Engineers airborne Lidar bathymetry (ALB) survey data into NOAA's processing workflow. NOAA, DOI: 0.7289/V5/TM-NOS-CS-36
- Wozencraft, Jennifer M.; W. Jeff Lillycrop (2003): SHOALS airborne coastal mapping: Past, present, and future. *Journal of Coastal Research*, Special Issue, 38, pp. 207–215
- Wright, C. Wayne; Christine Kranenburg et al. (2016): Depth calibration and validation of the experimental advanced airborne research Lidar, EAARL-B. *Journal of Coastal Research*, DOI: 10.2112/si76-002
- Zhang, Keqi; Dean Whitman et al. (2005): Quantification of beach changes caused by hurricane Floyd along Florida's Atlantic coast using airborne laser surveys. *Journal of Coastal Research*, DOI: 10.2112/02057.1
- Zhao, Xinglei; Jianhu Zhao et al. (2018): Remote sensing of suspended sediment concentrations based on the waveform decomposition of airborne LiDAR bathymetry. *Remote Sensing*, DOI: 10.3390/rs10020247

Klein und stark.

UNSERE USBL-FAMILIE WÄCHST



Gaps M5

Exportfreies omnidirektionales - Unterwasser-navigationssystem – von der Oberfläche bis in mittlere Gewässertiefen (995 m) einsetzbar.

iXblue

oceanology
international
Booth #E100